ARTICLE

Elastic Low-Energy Electron Collisions with Methanethiol

Ke-dong Wang[a,b*], Ju Meng[b]

a. Institute of Theoretical and Computational Chemistry, Key Laboratory of Mesoscopic Chemistry of MOE, School of Chemistry and Chemical Engineering, Nanjing University, Nanjing 210093, China
b. School of Physics and Electronical Engineering, Henan Normal University, Xinxiang 453007, China

We report *ab initio* scattering calculations results of electron-methanethiol collisions using R-matrix approach within the static-exchange and static-exchange-polarization approximations. The calculated elastic integral cross sections are in agreement with the experimental data. Two shape resonances of $^2A'$ symmetry located at 4.06 and 8.32 eV are detected within static-exchange-polarization model. For this dipole molecule, Born-closure procedure was used to account for the higher partial waves ($l>4$) for the convergence of the cross section. The effective collision frequencies over a wide electron temperature range ($200-30000$ K) are calculated using the data of the momentum-transfer cross section.

Key words: Elastic integral cross sections, Differential cross section, Shape resonance

I. INTRODUCTION

Electron collisions with molecule are important in investigating physic-chemistry of interstellar, environmental media and plasma-based processing. The study of low-energy electron scattering from biological molecules helps to understand the effect of radiation on biological systems [1]. Electron-driven processes on methanethiol are observed to happen in Earth's atmosphere and in interstellar space [2]. It is also applied to chemical industry as well as in the field of biochemistry. As one of the most important products of degradation of organic matter, methanethiol is mainly used to produce methionine [3].

Experimental studies on the electron-assisted processes involving methanethiol in the gas phase has also been studied. In early experiments, Jäger and Henglein [4] investigated dissociative electron attachment (DEA) to methanethiol. Amos *et al.* [5] investigated the positive-ion formation. Dezarnaud *et al.* [6] studied the lower energy ($0-7$ eV) transmission measurements of methanethiol. They discerned a broad shape-resonance centred at 2.85 eV and suggested that the extra electron was temporarily trapped in σ^* molecular orbitals localized on the $C-S-H$ linkage. Subsequently, Szmytkowski *et al.* measured the absolute cross section of methanethiol in a linear electron-transmission experiment [7]. They suggested that there were two resonant peaks: one weak peak around 4 eV and the other one around 8 eV. Recently, Limbachiya *et al.* calculated total cross sections for methanethiol on electron impact

for energies from 10 eV to 5000 eV [8]. Theoretical work concerning the low-energy electron collision with methanethiol molecule below the electron energy 10 eV has not been available yet.

In this work, we calculate the elastic integral cross sections for methanethiol in the electron energies ranging from 0.01 eV to 10 eV. During the course of electron-molecule scattering, the formed shape resonances which can cause enhancements in the cross sections are explored. The electron-scattering calculations are performed at static-exchange (SE), static-exchange-polarization (SEP) using UK molecular R-matrix code [9, 10], which has been proven to be a reliable method to study electron scattering in the low energy region [11–14]. The integrated elastic, differential, and momentum cross sections for electron impact on the methanethiol molecule are reported.

II. METHOD

A. Theory

The molecular R-matrix method [15, 16] is a variational technique that relies on the partitioning of configuration space into an inner and an outer part. The boundary is a sphere whose center is located at the center of mass of the molecule. The radius is chosen so that the molecular electron cloud is fully contained within the sphere. In the inner region, exchange and electron-electron correlations are considerable. As a result, the collision problem within a finite volume can be treated as a molecular bound state problem, by constructing and diagonalizing a Hamiltonian matrix. To meet the boundary conditions, the Bloch operator is added to the diagonalized inner region Hamiltonian. In the outer

───────
*Author to whom correspondence should be addressed. E-mail: wangkd@htu.cn

region, exchange and electron-electron correlations are not important and are negligible, and one need only account for the long-range multi-polar interactions between the scattering electrons and the target. Hence the problem can be simplified to solve a set coupled second order equations, which is in practice done by propagating the R-matrix and matching to the asymptotic expansion of the solution to obtain the scattering observables.

In inner region, the wave function of the scattering system is written using the configuration interaction expression

$$\Psi_k^{N+1} = A \sum_{ij} a_{ijk} \Phi_i^N (x_1, \cdots, x_N) u_{ij} (x_{N+1}) +$$
$$\sum_i b_{ik} \chi_i^{N+1} (x_1, \cdots, x_{N+1}) \quad (1)$$

where A is an antisymmetrization operator, x_N is the spatial and spin coordinate of the Nth electron, Φ_i^N represents the ith state of the N-electron target, μ_{ij} is a continuum-orbital spin coupled with the scattering electron, and k refers to a particular R-matrix basis function. Coefficients a_{ijk} and b_{ik} are variational parameters determined as a result of the matrix diagonalization. The sum in the second term of Eq.(1) represents the short-range correlation and polarization effects, running over all configurations χ_i^{N+1} that are L^2 functions. These are also important for relaxing the orthogonality imposed between the target and continuum orbitals. Gaussian-type orbitals (GTOs) were used to represent the target molecular orbitals.

B. Target and scattering models

Methanethiol is a close shell molecule with C_s symmetry in its equilibrium geometry, its ground state is $^1A'$ electronic state. The geometry ($R(C-S)$=1.815 Å, $R(S-H)$=1.343 Å, $\angle C-S-H$=96.662°) optimized at MP2/6-31+G** level are employed in the present calculations. We calculate the target state with the 6-31G, 6-311G, cc-pVDZ and cc-pVTZ basis sets, and target wave functions based on Hartree-Fock method with cc-pVDZ Gaussian type orbital basis set predict the best target state. It gives a ground state energy of −437.7255 Hartree and predicts a permanent dipole moment of 1.65 D which is in good agreement with the experimental value of 1.52 D [17]. Two different R-matrix radii $12a_0$ and $15a_0$ are used to test the calculations.

The calculations are performed at SE and SEP levels: only the ground state of the target, described at the HF level, is included in Eq.(1). The SE model can only give shape resonances that are usually too high in energy. The SE model is a well defined approximation which makes the cross comparison between calculations straightforward and meaningful. In the SEP
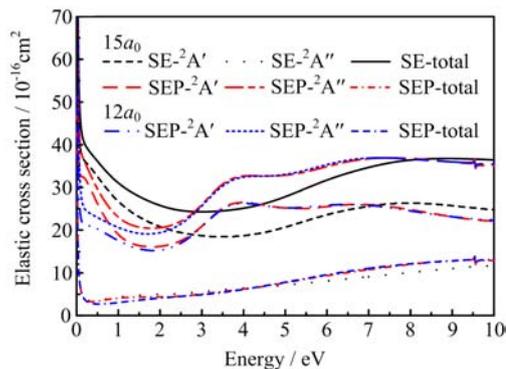

FIG. 1 Elastic cross sections of the electron impact on the methanethiol molecule in the SE and SEP models.

model, singlet excitations out of the HF wave function are used to represent target polarization effects. It can give the good resonance parameters for the shape resonant states. In the present calculations, the L^2 configurations in Eq.(1) associated with this model can be written in two classes, $(core)^4(valence)^9(virtual)^1$ and $(core)^4(valence)^8(virtual)^2$. In the present SEP model 20 MOs of A' symmetry (11a'-30a') and 7 MOs of A'' symmetry (4a''-10a'') are selected as virtual orbitals. The continuum orbitals up to l=4 (g-partial waves) are represented by GTO. The partial waves for l>4 are included using a Born correction via a closure approach [18] at all energies. No more resonant states are predicted here because the configuration wave functions at the higher states (such as core-excited Shape or Feshbach resonant states) are not explicitly considered.

III. RESULTS AND DISCUSSION

A. Elastic integral cross sections

In Fig.1 we present our calculated elastic integral cross sections of methanethiol in SEP models based on the cc-pVDZ basis set at different R-matrix radii $12a_0$ and $15a_0$. Although both of them predict the similar shape of total integral cross section, there are slight differences existing especially in the low energy <2.5 eV. This indicates that R-matrix radius $15a_0$ is better to contain the molecular electron cloud and be used in the present calculations. As shown in Fig.1, the different total cross sections between SE and SEP are mainly from the $^2A''$ symmetry because both SE and SEP models predict almost the same $^2A'$ cross section. The total cross section of SE model shows a hump from 6.5 eV. We find that this hump is mainly due to the resonance at 7.60 eV arising from $^2A'$ symmetry with a width of 3.5 eV. For lack of polarization effects in the SE approximation, the position of the resonance is much higher in energy than that observed in the experiment [7]. This resonance is usually called σ^* resonance since the in-
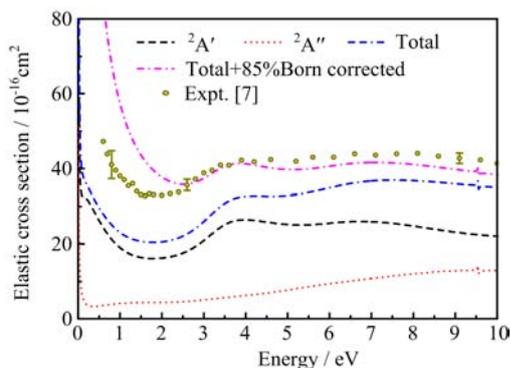
FIG. 2 SEP integral cross sections, Born corrected cross section of methanethiol with experimental total cross section from Szmytkowski *et al.* [7] for comparison.

FIG. 3 Our calculated eigenphase sums at R-matrix radii $15a_0$ with SEP model.

cident electron is captured in a virtual σ^* MO. The position of the σ^* resonance goes down to 4.06 eV for our SEP model, which is in agreement with the experimental value of 4 eV.

Figure 2 shows the SEP integral cross sections and experimental total cross section from Szmytkowski *et al.* [7] for comparison. There is a broad enhancement of the SEP integral cross section starting from 3.0 eV. The hump between 3.0 and 10.0 eV indicates that there are some broad resonances in the region. By analyzing the two components ($^2A'$ and $2A''$) of the total elastic cross section, we find the hump comes from the $^2A'$ symmetry. Through fitting the eigenphase sum to a Breit-Wigner profile [19, 20], one usually can obtain the energy position and the width of the resonance. Our calculated eigenphase sums at R-matrix radii $15a_0$ are shown in Fig.3. The increase of the eigenphase sum for about π radians in a (generally) narrow energy range usually characterizes the scattering resonances. The eigenphase sum indicates there are two σ^* shape resonances of $^2A'$ symmetry located at 4.06 and 8.32 eV. Their widths are 2.0 and 3.5 eV with the configurations of $1a'^2\text{-}10a'^2 1a''^2\text{-}3a''^2 11a'$ and $1a'^2\text{-}10a'^2 1a''^2\text{-}3a''^2 12a'$, respectively. Szmytkowski *et al.* [7] suggested that there were two weakly differentiated peaks in their measured total cross section: a weaker one around 4 eV and a more prominent one near 8 eV. Our calculations are in good agreement with their conclusions.

To obtain converged cross sections, the effect of rotation can be included along with a very large number of partial waves using closure approach [18]. Considering the overestimation of the dipole momentum in the calculations and the cross section of Born correction proportional to square of the dipole momentum in the Born corrections, we include 85% of the calculated Born corrections in the total elastic cross section in Fig.2. Born corrected cross section is obviously higher than the measured data in the low-energy region <2.5 eV and slightly lower in the region >4.5 eV. Methanethiol, just like water [21] and methyleneimine [12], is a strongly
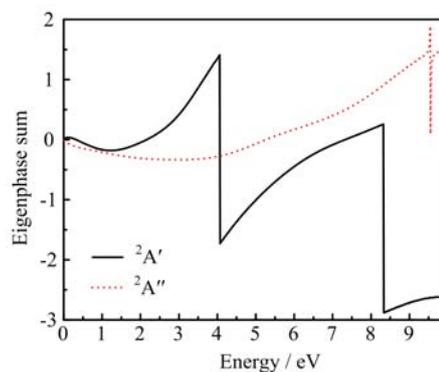
polar molecule which means that, particularly at low electron collision energies, its differential cross section is very heavily forward peaked. This makes the direct measurement of integral cross sections very challenging because of the difficulties associated with making measurements at low angles. So it is reasonable that Born corrected cross section is higher than the measured data in the low-energy region <2.5 eV.

B. Differential cross sections

By processing K matrices which is obtained before, DCS is achieved by using the POLYDCS program [22]. The calculated dipole moment (1.65 D), the experimental dipole moment (1.52 D) [17] and the rotational constants A=3.477 cm^{-1}, B=0.432 cm^{-1} and C=0.414 cm^{-1} at the equilibrium geometry of the ground state of the molecule are used to evaluate the DCS. The DCSs for elastic scattering of methanethiol by electron impact are calculated in the energy range of $0.01-10$ eV and at scattering angles of $0°-180°$.

Figure 4 shows the DCS at the electron energies of 1, 2, 4, 6, 8, and 10 eV. The DCSs at all the energies show the sharp increases at the smaller scattering angles for the dipolar nature of the target. The DCS at 1 eV appears a minimum at about $150°$. This minimum of the DCS gradually reduces to $90°$ with the incident energy increasing to 10 eV. The rotationally resolved DCSs at the incident energy of 2 eV are shown in Fig.5. The $0{\rightarrow}1$ contribution dominates for scattering angles less than $60°$. At the angles more than $120°$, $0{\rightarrow}2$ component contribution is the largest. As shown in the figure, the contribution of the higher J' decreases with the J' increases, and the convergent results are obtained when J' increases up to 5.

Our calculated momentum-transfer cross section (MTCS) is shown in Fig.6. As might be expected from the DCSs, it shows a broad peak between 3 and 9 eV. As discussed before, it is due to two σ^* shape resonances of $^2A'$ symmetry located at 4.06 and 8.32 eV.
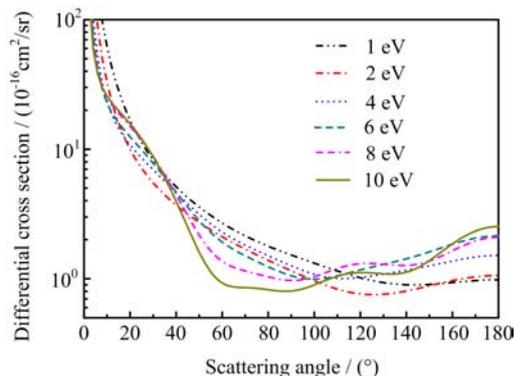
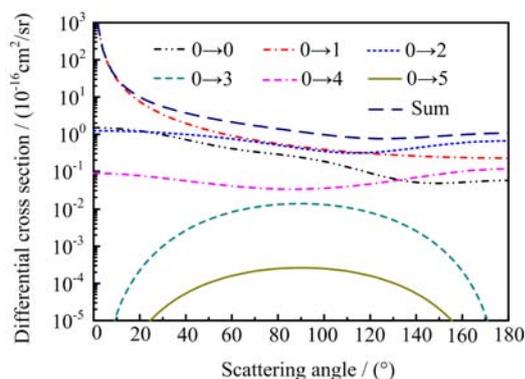FIG. 4 Differential cross section (DCS) of methanethiol at different energies of 1, 2, 4, 6, 8 and 10 eV.

FIG. 5 Electron impact R-matrix rotationally re-solved state-to-state $(J \to J')$ differential cross sections of methanethiol at 2 eV.

FIG. 6 Momentum transfer cross sections of methanethiol for energy range of $0.01-10.00$ eV.
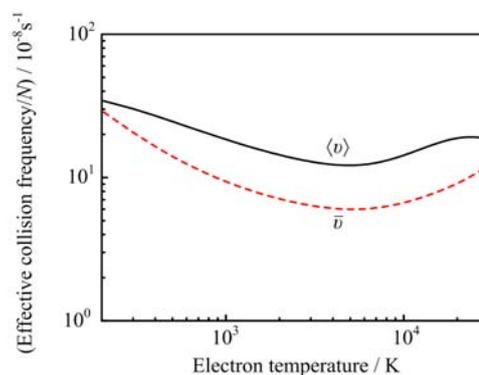
FIG. 7 Effective collision frequency of the methanethiol molecule ground state.

MTCS doesn't exhibit singularity in the forward direction due to the multiplicative factor $(1-\cos\theta)$, where θ is scattering angle. Based on the present MTCS data, two types of the effective electron-methanethiol collision frequency $\langle \nu \rangle$ and $\bar{\nu}$ [23] are evaluated. These are given by the following expressions:

$$\langle v \rangle = \frac{8}{3\pi^{1/2}} N \left(\frac{m_e}{2k_B T_e} \right)^{5/2} \int_0^\infty v^5 Q^m(V) \cdot$$
$$\exp(-\frac{m_e v^2}{2k_B T_e}) \mathrm{d}v$$
$$\frac{1}{\bar{v}} = \frac{8}{3\pi^{1/2} N} \left(\frac{m_e}{2k_B T_e} \right)^{5/2} \int_0^\infty \frac{v^3}{Q^m(v)} \cdot$$
$$\exp\left(-\frac{m_e v^2}{2k_B T_e} \right) \mathrm{d}v \qquad (2)$$

Here, N is the number density of molecules, m_e is the electron mass, k_B is the Boltzmann factor, T_e is the electron temperature, v is the velocity of the electron, and $Q^m(v)$ is the velocity-dependent MTCS. The effective collision frequency are plotted in Fig.7. The collision frequencies are related to transport properties like mean-free path, mobilities, and diffusion coefficients.
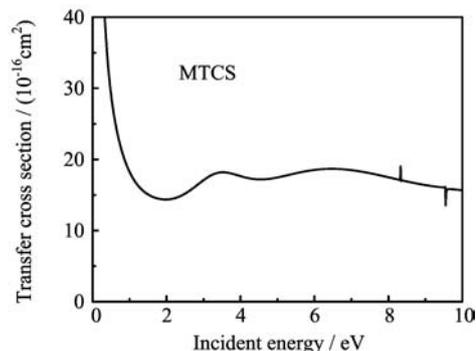
IV. CONCLUSION

We have calculated the elastic electron-scattering cross section for methanethiol molecule using R-matrix method in SE and SEP approximation. The calculated total cross section shows a hump between 3 and 10 eV. Our calculated eigenphase sum suggests that there are two σ^* shape resonances of $^2A'$ symmetry located at 4.06 and 8.32 eV in this region with a width of 2.0 and 3.5 eV, respectively, which are in agreement with the conclusions from Szmytkowski *et al.* [7]. Born corrected total cross section is higher than the measured data in the low-energy region <2.5 eV and slightly lower in the region >4.5 eV. The DCS has been used to calculate the elastic momentum transfer cross section. The MTCS plays an important role in the energy distribution during collision. We have also presented rate coefficients for elastic processes up to 30000 K by assuming the Maxwellian distribution for the electrons.

V. ACKNOWLEDGMENTS

[1] B. Boudaïffa, P. Cloutier, D. Hunting, M. A. Huels, and L. Sanche, Science **287**, 1658 (2000)

[2] M. Hines and M. Morrison, J. Geophys. Res. **97**, 16703 (1992).

[3] J. Norell, R. P. Louthan, and P. Rector, *"Thiols". Kirk-Othmer Concise Encyclopedia of Chemical Technology*, 3rd Ed., New York: John Wiley & Sons, Inc., (1988).

[4] K. Jäger and A. Henglein, Z. Naturf. **a21**, 1251 (1966).

[5] D. Amos, R. G. Gillis, J. L. Occolowitzand, and J. F. Pisani, Org. Mass Spectrom. **2**, 209 (1969).

[6] C. Dezarnaud, M. Tronc, and A. Modelli, Chem. Phys. **156**, 129 (1991).

[7] C. Szmytkowski, G. Kasperski, and P. Mozejko, J. Phys. B **28**, L629 (1995).

[8] C. Limbachiya, M. Vinodkumar, M. Swadia, and A. Barot, Mol. Phys. **112**, 101 (2014).

[9] J. M. Carr, P. G. Galiatsatos, J. D. Gorfinkiel, A. G. Harvey, M. A. Lysaght, D. Madden, Z. Masin, M. Plummer, J. Tennyson, and H. N. Varambhia, Eur. Phys. J. D **66**, 58 (2012)

[10] J. Tennyson, Phys. Rep. **491**, 29 (2010).

[11] K. D. Wang, Y. P. An, J. Meng, Y. F. Liu, and J. F. Sun, Phys. Rev. A **89**, 022711 (2014).

[12] K. D. Wang, J. Meng, and K. L. Baluja, Eur. Phys. J. D **69**, 78 (2015).

[13] Y. F. Wang and S. X. Tian, Phys. Rev. A **85**, 012706 (2012).

[14] S. B. Zhang, J. G. Wang, R. K. Janev, and X. J. Chen, Phys. Rev. A **82**, 062711 (2010).

[15] P. G. Burke, *R-Matrix Theory of Atomic Collisions: Application to Atomic, Molecular and Optical Processes*, Berlin: Springer-Verlag, (2011).

[16] L. A. Morgan, C. J. Gillan, J. Tennyson, and X. Chen, J. Phys. B **30**, 4087 (1997).

[17] NIST 2008 Computational Chemistry Comparison and Benchmark Database, http://cccbdb.nist.gov/.

[18] S. Kaur, K. L. Baluja, and J. Tennyson, Phys. Rev. A **77**, 032718 (2008).

[19] J. Tennyson and C. J. Noble, Comput. Phys. Commun. **33**, 421 (1984)

[20] H. Friedrich, *Theoretical Atomic Physics*, 3rd Ed. Berlin: Springer, 47 (2006).

[21] H. Silva, J. Muse, M. C. A. Lopes, and M. A. Khakoo, Phys. Rev. Lett. **101**, 033201 (2008).

[22] N. Sanna and F. A. Gianturco, Comput. Phys. Commun. **114**, 142 (1998)

[23] P. Baille, J. S. Chang, A. Claude, R. M. Hobson, G. L. Ogram, and A. W. Yau, J. Phys. B **14**, 1485 (1981).